Applied Thermal Engineering 69 (2014) 143e154

Con en s lis s a ailable a ScienceDirec

Applied Thermal Engineering

jo rnal homepage: .else ier.com/loca e/ap hermeng

Power generation with ORC machines using low-grade waste heat or renewable energy

Vasile Minea*

Hydro-Québec Research Institute, Laboratoire des technologies de l'énergie (LTE), 600, avenue de la Montagne, Shawinigan G9N 7N5, Canada

highlights

- A laboratory-scale beta-prototype Organic Rankine Cycle machine has been studied.
- Cycle efficiency with feed pump at variable full range speed has been determined.
- Energetic and exergetic conversion efficiencies have been experimentally evaluated.
- Various effects of evaporator superheating on the cycle efficiency have been analysed.
- Several cycle improvements and potential industrial application were identified.

article info

Article history:
Received 10 February 2014
Accepted 19 April 2014
Available online 28 April 2014

Keywords:
Industrial waste heat recovery
Renewable energy
Power generation
Organic Rankine cycle
Energy efficiency

abstract

By 2030, global energy consumption is projected to grow by 71%. At the same time, energy-related carbon dioxide emissions are expected to rise by more than 40%. In this context, waste and renewable energy sources may represent alternatives to help reduce fossil primary energy consumption. This paper focuses on the technical feasibility, efficiency and reliability of a heat-to-electricity conversion, laboratory beta-prototype, 50 kW Organic Rankine Cycle (ORC) machine using industrial waste or renewable energy sources at temperatures varying between 85 °C and 116 °C. The thermodynamic cycle along with the selected working fluid, components and control strategy, as well as the main experimental results, are presented. The study shows that the power generated and the overall net conversion efficiency rate of the machine mainly depends on such parameters as the inlet temperatures of the waste (or renewable) heat and cooling fluid, as well as on the control strategy and amount of parasitic electrical power required. It also indicates that after more than 3000 h of continuous operation, the ORC-50 beta-prototype machine has shown itself to be reliable and robust, and ready for industrial market deployment.

1. Introduction

In Canada, eight major manufacturing sectors account for over 91% of the energy input to the manufacturing industries and about 71% of the input energy is released to the environment via four classes of identifiable waste heat streams at relatively low temperatures (i.e. up to 370 °C) in the form of stack gases, vapour or liquid effluents [1]. Such energy rejections along with power generation from fossil fuel combustion lead to global warming and ambient air pollution. Generally, heat recovery below 370 °C is not economically feasible for producing electricity with conventional steam-based power generation cycles such as Diesel, Stirling, or basic ClausiuseRankine. The last of these, for example, converts heat into work at higher temperatures by using water as a working fluid, but it becomes inefficient at input temperatures below 370 °C [2]. Consequently, different energy conversion techniques are required to efficiently use low-grade "free" waste heat resources for power generation [3e6]. Among these alternatives, Organic Rankine Cycle-based (ORC) machines, similar to basic Clausiuse Rankine power plants, do not use water, but rather vaporize high-molecular-mass fluids (also known as organic fluids) with boiling points below that of water [7,8]. ORC machines can use various types of low-grade industrial waste heat or renewable (solar, biomass, geothermal) energy sources. But, in spite of their well-known advantages over conventional high-temperature water steam cycles (e.g. lower operating pressures and temperatures, smaller size, and lower complexity and costs), ORC machines have not been widely used so far, mainly because of concerns about their economic feasibility, lower heat-to-power conversion efficiency, and, in certain cases, parasitic energy consumptions.

* Tel.: +1 819 539 1400 (1507); fax: +1 819 539 1409.
E-mail address: minea.vasile@lte.ireq.ca.

http://dx.doi.org/10.1016/j.applthermaleng.2014.04.054
1359-4311/

2. Experimental set-up

A 50 kW beta-prototype ORC machine was designed, built [9], and installed on a laboratory test bench [10e12]. The prototype includes a single-stage twin screw expander, a stainless steel condenser and pre-heater/evaporator heat exchanger assembly, a liquid receiver, and a working fluid variable speed circulation pump (WFP) (Fig. 1). The machine is scalable, allowing for the connection of multiple similar units to a single heat source if enough energy is available. If these units are installed in parallel, enough hot water flow rate for each machine is needed. If they are connected in series with one using hot water from the pre-heater outlet of the other, the heat source entering temperature will need to be high enough, as well.

Routine maintenance is easy, and with a basic set-up, technicians with an HVAC and mechanical background can handle required maintenance. Additionally, the control system is fully automated, allowing for remote control and monitoring via an Internet connection, as well as off site maintenance. The small footprint, skid-mounted ORC-50 machine has been connected to a 700 kW electrical boiler, simulating the waste (or renewable) heat source, to an air-cooled liquid cooler, and to the Hydro-Québec electrical grid. The machine converts into electrical power the thermal energy recovered from the waste (or renewable) heat entering the machine in a liquid form (water) at temperatures varying from 85 °C up to 125 °C. The ORC-50 machine's output power ranges from 20 to 50 electrical kW, depending on the inlet temperatures and flow rates of the source and sink heat sources, respectively.

The system was comprehensively instrumented with thermocouples, power and pressure transducers, flow meters for the working fluid, and both organic fluid, heat source, and sink thermal carriers. A data transmission system and associated analysis software were set up to monitor system operation. All parameters were scanned at 15 s intervals, then averaged and saved every minute, to help determine the cycle's instantaneous and overall thermodynamic performance.

2.1. Thermodynamic cycle

The low-pressure (p_1) organic fluid leaving the condenser as a saturated or sub-cooled liquid (state 1) accumulates inside the receiver in equilibrium with its vapour phase (see Figs. 1 and 5). Then it enters the working fluid feed pump (WFP) where its pressure is adiabatically raised to the saturation (evaporating) pressure (p_2) (state 2s), prior to entering the pre-heater/evaporator heat exchanger assembly. The multistage feed pump is driven by a variable frequency drive (from 0 to 60 Hz) in order to supply the flow rate required to achieve a relatively small superheating effect (i.e. below 5 °C) at the evaporator outlet [13]. Also, between 10% and 15% of the organic fluid flow rate leaving the feed pump is injected into the expander at both the inlet and outlet ports.

Since the exergy destruction rate in the feed pump is relatively small, the 1e2s process is considered as isentropic (adiabatic), and the power input is expressed as

$$W_p = \frac{W_{p,ideal}}{\eta_p} = \frac{\dot{m}_{OF}(h_{2s} - h_1)}{\eta_p} = \frac{\dot{m}_{OF}(p_2 - p_1)}{\rho\eta_p} \quad (1)$$

where $W_{p,ideal}$ is the feed pump ideal power input (kW), η_p e the feed pump isentropic efficiency (90%), $\dot{m}_{OF}$ e the organic fluid mass flow rate (kg/s), h_1 and h_{2s} e the organic fluid mass enthalpies at the inlet and outlet ports of the feed pump in the ideal case, respectively (kJ/kg), p_1 and p_2 e the organic fluid pressures entering and leaving the feed pump, respectively, and ρ e the organic fluid average mass density (kg/m^3). On the other hand, the waste heat fluid carrier (water) enters the evaporator where it transfers heat to the working fluid during the evaporation and superheating processes (3e4e5). At the evaporator outlet, approximately 20% of the waste heat fluid (water) flow rate enters the pre-heater to partially or completely preheat the organic fluid from the sub-cooled liquid state (2s) up to (near) the saturated state (2a). The preheated organic fluid enters the evaporator at state 2a where it will vaporise and superheat at a constant pressure (process 2ae3e4e5). The pre-heater/evaporator thermal power recovered from the waste heat source is given by

$$Q_{pre-heat/ev} = \dot{m}_{OF}(h_5 - h_{2a}) \quad (2)$$

where h_5 and h_{2a} are the organic fluid mass enthalpy leaving and entering the pre-heater/evaporator, respectively (kJ/kg). The pre-heater/evaporator assembly was designed and selected to optimally work with hot water flow rates in the range of 7.6e12 l/s (120e200 GPM). Its thermal efficiency versus size and cost was carefully analysed in order to achieve optimum pinch points defined as the differences between the corresponding waste heat (source) temperature and the temperature at which the organic fluid begins to vaporize [9].

The high-pressure saturated (state 4) or superheated vapour (state 5) leaving the evaporator enters the twin screw expander. It

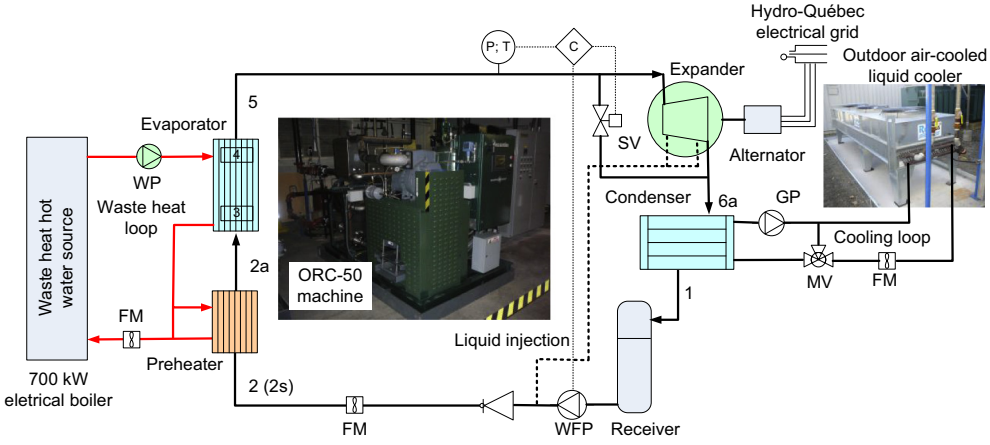

Fig. 1. Schematic representation of the experimental setup [9e11]. C e controller; FM e flow meter; GP e cooling fluid (water/glycol) pump; MV e mixing valve; P e pressure; T e temperature; WP e waste heat thermal carrier (water) pump; WFP e working fluid pump; SV e solenoid valve.

accelerates a 50 kW (460 V) asynchronous induction generator (alternator) connected to the local electrical grid. Control of the evaporator exit dryness fraction is achieved with a microprocessor that generates signals from the pressure and temperature inputs to vary the feed pump speed and thus provide proper superheat levels [14]. Inside the screw expander, the working fluid expands creating pressure and temperature drops at the exit port, thus converting the thermal energy of the high pressure vapour into mechanical work. Without any liquid injection, the organic fluid would leave the expander at state 6 but, because of this process, it actually leaves the expander at state 6a, closer to the vapour saturated wet curve. Fig. 5 shows that the increased wetness of the organic fluid at the expander inlet reduces the superheat at its exit port. As the vapour wetness at the expander inlet increases, it even allows the working fluid to leave the expander as wet vapour. Since less heat is required per unit mass flow to evaporate the working fluid only partially, given the same heat supply, the mass flow rate of the organic fluid is thus increased. Also, reducing the need for desuperheat after expansion tends to increase the specific enthalpy drop in the expander. Both these effects tend to increase power output. The actual expansion process (5e6) in the expander is a non-isentropic, non-reversible process which allows for dry expansion, thus preventing the vapour from condensing or forming droplets. The entropy increases, thus decreasing the power generated when compared with the ideal (isentropic) process 5e6s. This means that the efficiency of the heat-to-electricity transformation process in the expander could never reach its full value (100%).

During machine start-up, the asynchronous induction generator is first mechanically brought to near its synchronous speed (1800 rpm for 60 Hz) via the expander. For less than 100 ms there is a small inrush current spike at grid connection, but not higher than the generator's Locked Rotor Amps. Then, the generator is connected to the grid being driven slightly above the synchronous speed (i.e. at about 1840 rpm for 60 Hz). Integral power factor correction capacitors are used to improve the inherently low power factor of the induction alternator. In the event of a grid loss, the unit will automatically shut down, and cannot be re-started until line conditions return to normal [8].

The power generated by the twin screw expander can be calculated with one of the following formulas:

$$W_{exp} = W_{exp,ideal} * \eta_s \eta_m = \dot{m}_{OF}(h_5 - h_{6s})\eta_s \eta_m = \dot{m}_{OF} c_p \eta_s T_5 \left[1 - \pi^{\frac{1-\gamma}{\gamma}}\right] = \frac{2\pi n}{60} \Gamma \quad (3)$$

where $W_{exp,ideal}$ is the expander ideal power, $\eta_s = (h_5 - h_6)/(h_5 - h_{6s})$ e the expander isentropic efficiency (see Fig. 5), η_m e the mechanical efficiency, h_5 and h_{6s} e the working fluid enthalpies at the inlet and outlet ports of the expander in the ideal case, respectively (kJ/kg), c_p e the isobaric specific heat (kJ/kgK), T_5 e the expander inlet temperature (°C), π e the expander pressure ratio (p_5/p_6), n e the rotation speed of the expander shaft, γ e the polytropic exponent, and Γ e the expander torque. Generally, the isentropic efficiency of turbines/expanders can reach 80% [15,16], but for such a relatively small twin screw expander, a design isentropic efficiency (η_s) of 70% has been considered reasonable [12]. The 40 HP/460 V asynchronous alternator of the ORC-50 machine is linked to the 25 kV Hydro-Québec electrical grid via a 25 kV/600 V transformer with a nominal power of 2.5 MVA.

The working fluid enters the condenser at state 6a, closer to its saturated state, where it is condensed at constant pressure and temperature (process 6a-1) to become a saturated or sub-cooled liquid (state 1). The condensing (latent) heat (enthalpy) is transferred from the vapour to the cooling fluid circulating within a water/glycol (50% by weight) closed loop linked to an air-cooled liquid cooler (see Fig. 1). The condenser thermal power is expressed by the following equation:

$$Q_{cd} = \dot{m}_{OF}(h_{6a} - h_1) \quad (4)$$

where h_{6a} and h_1 are the organic fluid mass enthalpies entering and leaving the condenser (kJ/kg). The cooling fluid flow rate in the condenser varies between 11.68 and 14.28 l/s (180e220 GPM) in order to keep the pre-set inlet temperatures constant between 15 °C and 30 °C. The condensed organic fluid at state 1 is stored inside the liquid receiver, pumped back to the pre-heater/evaporator assembly, and then a new cycle begins. The organic fluid pressure drops within the condenser, pre-heater and evaporator to about 30, 10 and 20 kPa, respectively.

2.2. Working *fluid*

Depending on the operating temperature ranges of ORC machines, the proper selection of the organic fluid may help reduce cycle thermodynamic inefficiencies and achieve higher energy conversion efficiency rates and lower capital costs [14].

Several fluids such as HCFC and HFC pure and azeotropic mixture refrigerants [16,17], benzene and toluene [18], were considered in the past as working fluids for low- and medium-temperature ORC cycles. For the ORC-50 machine under study, the HFC-245fa refrigerant, which has a lower boiling point than water, a relatively high molecular mass, and a high enough critical temperature (154 °C), was selected as a dry organic fluid. The main characteristic of such a fluid is that the slope of its saturation vapour curve is positive, which allows for dry expansion, thus preventing the vapour from condensing or forming droplets. HFC-245fa is also a low-pressure, high-temperature, non-corrosive, non-flammable, low-toxicity, and environmentally safe fluid. Its Ozone Depletion Potential (ODP) and Global Warming Potential (GWP) are 0 and 1900, respectively, and it has a B1 ASHRAE safety classification [19].

It also meets other operational, thermo-physical and environmental requirements, as a high stability, to avoid chemical deterioration and decomposition at the highest operating temperature, and low toxicity, explosion and flammability characteristics [20]. It must be safe (for human health), non-corrosive, compatible with common engine materials and lubricating oils, and available at affordable costs [21]. Organic fluids must also have a high density and latent (vaporization) heat to absorb more energy from low-grade waste heat sources, and thus provide higher power outputs. Another important parameter is the fluid critical point, which has to be above 300 K (~27 °C) in order to be able to reject heat into the ambient air during the condensation process.

2.3. Expander

Since standard turbines may rotate at very high speeds at low power output levels, requiring high ratio reduction gearboxes and relatively expensive lubrication systems [22,23], the ORC-50 prototype was equipped with a patented twin screw expander with simple bearing lubrication [8]. It operates at low speeds and is directly coupled via a belt to an asynchronous alternator (generator) without any intermediate reduction gearbox, which provides efficiency advantages over conventional turbines [13,14,24,25].

The patented twin screw expander consists of a pair of meshing helical rotors located inside a casing. The spaces between the lobes and the casing form together a series of rotating chambers. When the organic fluid is admitted, its volume will increase, while power is transferred between the fluid and the rotor shafts from the torque created by the forces acting on the rotor surfaces due to the

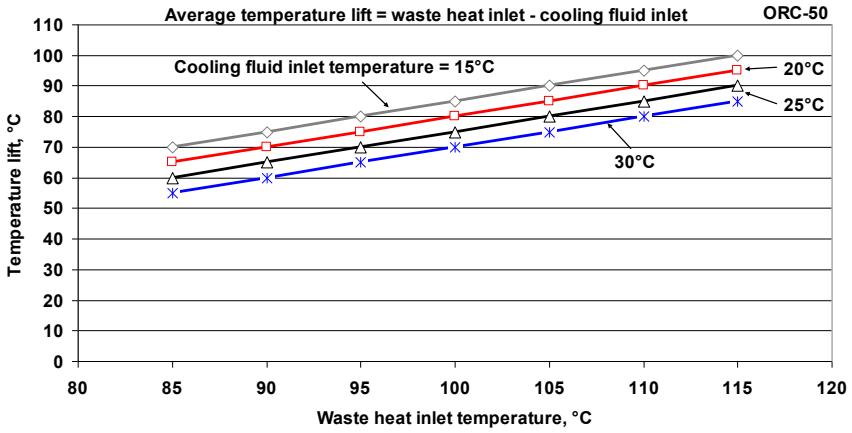

Fig. 2. Average difference (or cycle temperature lift) between the waste heat and cooling fluid inlet temperatures.

pressure. Only a relatively small portion of the power transferred is due to the dynamic effects associated with fluid motion. The expander can run in wet conditions, which means that the inlet refrigerant does not have to be 100% superheated vapour. The presence of liquid, together with the vapour or gas being expanded, has therefore little effect on its operation and efficiency. Moreover, since the liquid seals the gaps between the rotors and the casing, the lubrication process is enhanced [13,14,24,25]. The main lubrication system consists in dispersing up to approximately 5% oil by mass in the organic fluid [26]. The oil is transported by the liquid organic fluid through the evaporator and then through the expander, where it lubricates the rotors as the liquid working fluid dries during the expansion process. Also, as previously noted, some of the liquid organic fluid leaving the feed pump, prior to entering the evaporator, are distributed to the expander bearings where the frictional heat will evaporate it, leaving sufficient oil to lubricate them. This arrangement eliminates the need for any oil separator, storage tank, filters, cooler and circulating pump, usually required for conventional oil-flooded expander lubrication systems. This integrated lubrication method yields lower maintenance costs and reduces the total cost of the expander by roughly 80% compared to standard steam power plants [14,27].

3. Experimental results

First, this section presents part of the experimental results obtained with the organic fluid feed pump running at variable speeds (theoretically, with current frequency varying between 0 Hz and 60 Hz) in order to get small amounts of superheat at the evaporator outlet. Second, in order to illustrate the importance of this control strategy, a number of representative results obtained with the feed pump operating at a constant speed (i.e. 37 Hz), are provided.

3.1. Full variable feed pump speed

Experimental tests of the organic fluid feed pump running at variable speed over whole theoretical range (i.e., between 0 and maximum 60 Hz) were conducted with the waste heat thermal carrier (water) and cooling fluid (glycol/water 50% brine) entering the ORC-50 machine at temperatures of 85e105 °C and 15e30 °C, respectively. Under these thermal boundary conditions, the ORC-50 machine's average temperature increases (i.e. the difference between the waste heat and cooling fluid inlet temperatures) varied between 55 °C and 100 °C (Fig. 2). The mass flow rate of the waste heat thermal carrier was kept constant at 11.2 kg/s (173 GPM), while the mass flow rate of the cooling fluid varied with the use of a motorized mixing valve MV (see Fig. 1) between 10 kg/s and 14.8 kg/s (155e228 US GPM), depending on the actual ambient air temperature and the preset inlet temperature of the cooling fluid. At waste heat inlet temperatures above 105 °C, the operating parameters and cycle performance were predicted based on the experimental empirical linear equations (see Table 1) as well as on simulation models developed by using the EES software. Under all these boundary conditions, the ORC-50 machine ran continuously for more than 3000 h, proving its long term mechanical reliability and endurance.

3.1.1. Cycle validation

The main parameters (pressures, temperatures, flow rates and electrical power) that were measured helped validate each thermodynamic cycle by using the actual thermo-physical properties of the organic fluid. As can be seen in Fig. 3a and b, both the pressure and temperature of the superheated vapour entering the expander at state 5 increased with the waste heat inlet temperature according to the empirical linear correlations shown in Table 1 for waste heat inlet temperatures between 85 °C and 115 °C, at a constant cooling fluid inlet temperature (20 °C) in this example. The expander operated with expansion ratios of around 8 (see Table 2).

Fig. 4a shows the profile of the organic fluid flow rate for another typical test at a constant cooling fluid inlet temperature (15 °C), the feed pump running at variable speeds. It can be seen that, by controlling the feed pump speed, the organic fluid flow rate increased with the waste heat inlet temperature according to the empirical linear correlation shown in Table 1. As a result, the vapour superheat at the evaporator outlet remained below 4e5 °C (Fig. 4b) allowing the dry organic fluid to be further superheated during the expansion process without affecting the cycle thermodynamic performance. Even without any evaporator superheating (i.e. with

Table 1
Experimental correlations with feed pump running at variable speeds (0e60 Hz).

Parameter	Empirical linear correlation[a]
Expander inlet pressure (kPa, r)	$p_5 = 16.369T^{IN}_{waste} - 810.76$
Expander inlet temperature (°C)	$T_5 = 0.7773T^{IN}_{waste} + 12.574$
Organic fluid mass flow rate (kg/s)	$m_{OF} = 0.0278T^{IN}_{waste} - 1.0643$
Net power output (kW)	$W_{net} = 0.7801T^{IN}_{waste} - 43.577$
Net conversion efficiency rate (%)	$\eta_{net} = 0.0745T^{IN}_{waste} + 0.0114$

[a] For waste heat inlet temperatures (T^{IN}_{waste}) between 85 °C and 116 °C, at a constant cooling fluid inlet temperature (20 °C).

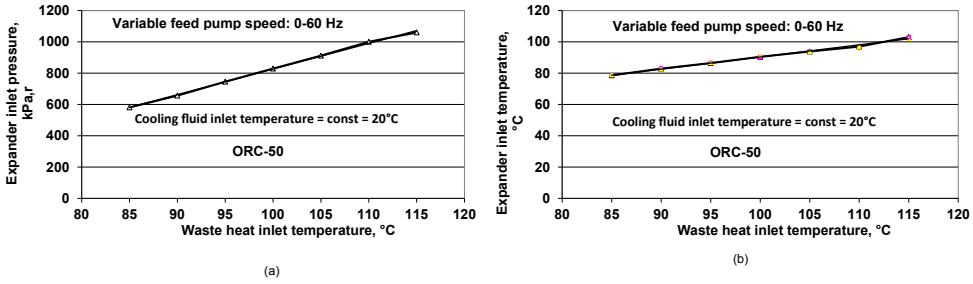

Fig. 3. Expander inlet pressure (a) and temperature (b) as functions of waste heat inlet temperatures at feed pump variable speed (0e60 Hz) and constant cooling fluid inlet temperature (20 °C); r: relative (gauge) pressure.

wet or saturated vapour at the expander inlet port), the machine would be able to operate correctly and provide maximum power output corresponding to the actual operating conditions [13].

Fig. 5a shows the thermodynamic cycle of a representative run (AD-14) with waste heat and cooling fluids entering the evaporator and condenser at constant temperatures of 105 °C and 20 °C, respectively. This test was achieved with an evaporator pinch point of about 3.5 °C and reasonable condenser sub-cooling (7.7 °C). It can be seen that, with an average mass flow rate of 1.93 kg/s, the temperature of the organic fluid at the evaporator exit did not exceed the critical temperature, and that the evaporator superheating was as low as 4 °C. Also, the actual temperature of the vapour leaving the expander (state 6a) was lower than the normal value (state 6) because of the colder liquid injected on both sides of the expander. Under these operating conditions, the net power output or the screw expander was 37.5 kW, i.e. about 75% of the maximum design power output of the ORC-50 prototype machine. The measured energetic balance of test AD-14 (Fig. 5b) was achieved with a net heat-to-electricity conversion energetic efficiency of 7.57% (see Section 3.1.3.1).

3.1.2. Net power output

The net power output of the ORC-50 machine was affected, among other parameters, by the waste heat and cooling fluid inlet temperatures, in other words, by the cycle temperature lift. Table 2 shows the extent to which the net power output depends on the expander inlet pressures and temperatures, expansion ratios, and cycle temperature lift at variable feed pump speeds (0e60 Hz) and a constant cooling fluid inlet temperature (20 °C).

Table 2 (and Fig. 6a) shows that the net power output increased linearly with waste heat inlet temperature, which varied from 85 °C to 115 °C, associated temperature lift (see Fig. 2), and organic fluid flow rates (see Fig. 4a) at all cooling fluid inlet temperatures (15, 20, 25, 25 and 30 °C). For example, with the cooling fluid entering the ORC-50 machine at 20 °C, the net power output increased from 19.2 kW to 43 kW (i.e. by 55.3%) when the waste heat inlet temperature increased from 85 °C to 115 °C. Also, with waste heat entering the ORC-50 machine at 100 °C, the net power output dropped from 35.9 kW to 29.8 kW, i.e. by about 17%, when the cooling fluid temperature increased from 15 °C (winter conditions) to 30 °C (summer conditions). In other words, by using waste heat at the highest available temperatures and higher temperature lifts, the ORC net power output could be proportionally improved. Conversely, for example, at the same waste heat source inlet temperature (90 °C), the expander electrical power output increased by about 28.3% (i.e., from 20.2 kW to 28.23 kW) when the cooling fluid inlet temperature dropped from 30 °C to 15 °C. This means that when the cooling water inlet temperature dropped by 1 °C, the power output increased by 4.7%.

Table 2
Net power outputs as functions of waste heat inlet temperatures and pressures increase.

Waste heat inlet temperature, T^{IN}_{waste} (°C)	Temperature increase, $T^{IN}_{waste} - T^{IN}_{cool}$ (°C)	Expander inlet pressure and temperature (see Fig. 5)		Expansion ratio, P_5/P_{6a}	Net power output, $\dot{W}_{net}$ (kW)
		p_5 (kPa, r)	T_5 (°C)		
85	65	581	79	7.71	22.3
90	70	656	83	8.0	26.4
95	75	745	86.4	8.2	31
100	80	830	91	8.3	35
105	85	911	94	8.4	39.9

Fig. 6b shows differently the impact of the cooling fluid inlet temperature on the net power output when the waste heat inlet temperature increased from 85 °C to 105 °C. It can be seen that, with a constant waste heat inlet temperature of 85 °C, the ORC-50 machine's net power output decreased by 19.4% when the cooling fluid inlet temperature increased from 15 °C to 30 °C. On the other hand, with the waste heat inlet temperature remaining constant at 105 °C, the net power output dropped by 12.3% when the cooling fluid inlet temperature increased from 15 °C to 30 °C.

3.1.3. Heat-to-electricity conversion efficiency

The vast majority of industrial applications of ORC machines involve irreversible processes in each component of the cycle that generate internal and external entropy. Among other effects, the process irreversibility makes it impossible to convert all of the available thermal energy into useful work and lowers the cycle overall efficiency [2]. Internal entropy generation is caused by friction (such as a pressure drop in the pipes) and unrestrained expansion (mainly in the expander), while external irreversibility is caused by heat transfers over finite temperature differences from hot to cold fluids (mainly in the pre-heater, evaporator and condenser), or by mechanical work transfers during the expander's expansion process.

The maximum reversible work that a given power cycle would be able to generate during a completely reversible process until it reaches a state in equilibrium with the surroundings (i.e. at same pressure and temperature with the environment), is known as exergy (or availability). A net entropy increase rate is related to the exergy destruction rate [2]. The degree of irreversibility (i.e. the decrease in exergy of the control mass plus the decrease in exergy of the heat transfer processes at the heat source's temperature minus the increase in exergy of the environment that receive the actual work) can thus be expressed in terms of the exergy destruction rate, which differs for each component of the ORC cycle.

For example, the evaporator and condenser, where the heat transfer processes aren't isobaric, make the largest contribution to the ORC cycle's overall exergy destruction rate, being the key

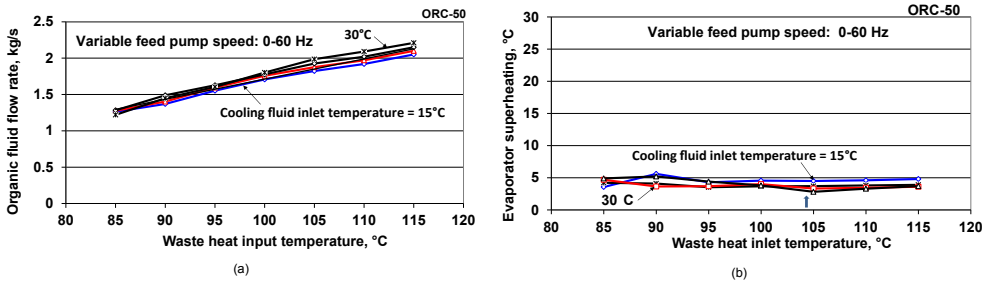

Fig. 4. Organic fluid flow rate (a) and superheating (b) as functions of waste heat and cooling fluid inlet temperatures, with feed pump operating at variable speed (0e60 Hz).

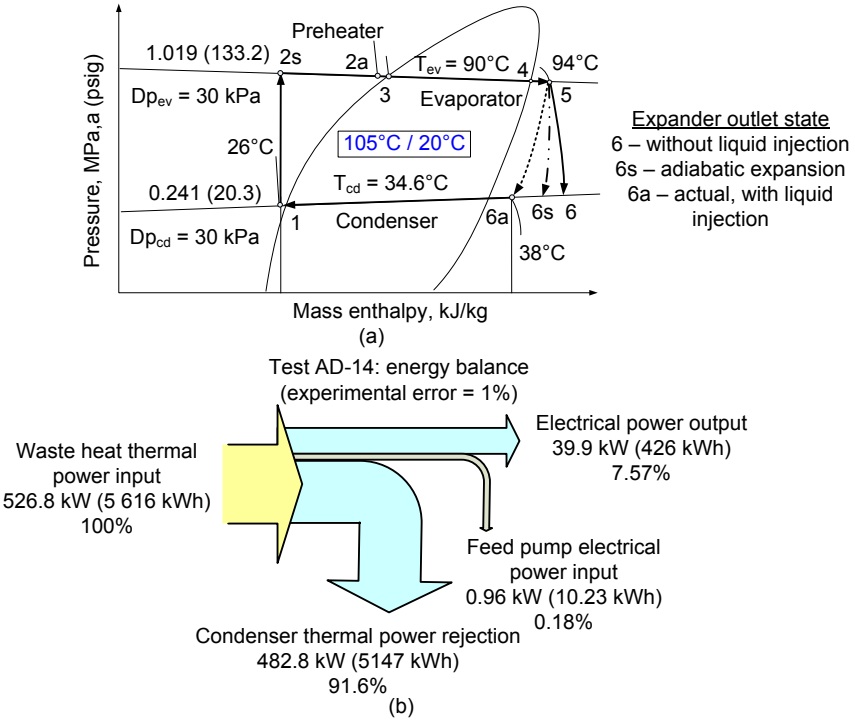

Fig. 5. (a) Typical thermodynamic cycle of test AD-14 using waste heat and cooling fluid inlet temperatures of 105 °C and 20 °C, respectively; (b) measured energetic balance; T_{cd}: condensing temperature; T_{ev}: evaporating temperature; Δp: pressure drop.

components causing irreversibility. Consequently, improving the evaporator and condenser design and thermal performance in order to reduce irreversibility is crucial in enhancing the ORC cycle's overall performance. The ORC machines using low-temperature heat sources require large evaporator and condenser heat transfer areas to extract the same amount of energy as high-temperature systems. This limits the use of low-temperature resources and emphasizes the necessity of optimum design and cost-effective ORC plants.

Exergy destruction also occurs during the non-isentropic expansion process. For a given waste (source) heat inlet temperature, as the inlet pressure and temperature of the organic fluid in the expander increase, the enthalpy drop increases and, correspondingly, the exergy destruction rate decreases, while the cycle

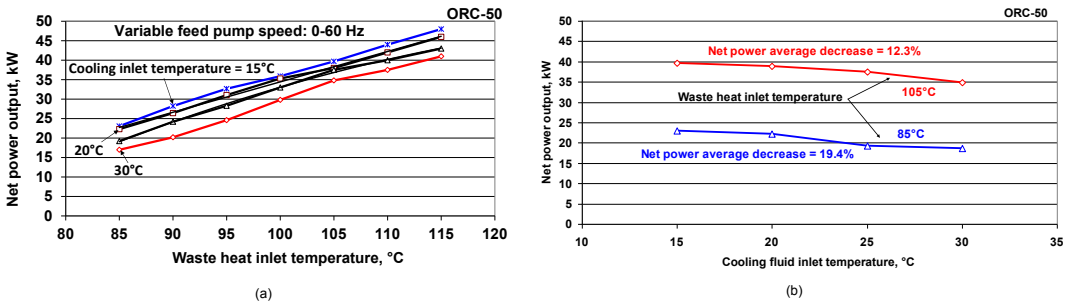

Fig. 6. (a) Net power output as a function of waste heat (a) and cooling fluid (b) inlet temperatures with the feed pump running at variable speed (0e60 Hz).

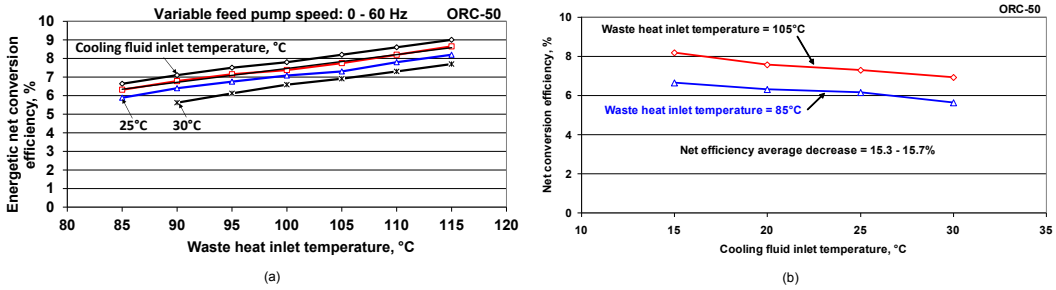

Fig. 7. Energetic net conversion efficiency as a function of waste heat thermal carrier (a) and cooling fluid (b) inlet temperatures with the organic fluid feed pump running at variable speed (0e60 Hz).

overall thermal efficiency increases. However, raising system pressure is not always feasible for economic reasons (e.g. higher capital costs and system complexity, materials selection, etc.).

3.1.3.1. Energetic conversion efficiency. The net heat-to-electricity energetic conversion efficiency rate (η_{net}) of ORC machines is a dimensionless number defined as the ratio of the net electrical power output ($W_{gross\text{-}exp} - W_{OFP}$) to the sum of the pre-heater ($Q_{pre-heat}$) and evaporator (Q_{evap}) thermal power inputs. It represents the fraction of thermal energy entering the ORC cycle that is converted into useful work. As the electrical power required by the feed pump was less than 3% of the expander power output, it has been ignored:

$$\eta_{net} = \frac{W_{net}}{Q_{tot-input}} = \frac{W_{gross-exp} - W_{OFP}}{Q_{pre-heat} + Q_{evap}} = \frac{(h_5 - h_{6s})\eta_s\eta_m}{(h_5 - h_{2s})} \quad (5)$$

where W_{net} represents the net electrical power output, i.e. the gross power produced by the expander ($W_{gross-exp}$) less the feed pump electrical power input (W_{ofp}); η_s e the isentropic expansion efficiency; η_m e the mechanical expansion efficiency. The heat added to the cycle can be expressed as

$$Q_{tot-input} = Q_{pre-heat} + Q_{evap} = \dot{m}_{waste}\left(h^{IN}_{waste} - h^{OUT}_{waste}\right) = \dot{m}_{waste}\bar{c}_{p,waste}\left(t^{IN}_{waste} - t^{OUT}_{waste}\right) \quad (6)$$

It can be seen in equation (5) that any parasitic electrical energy (or power) consumption, such as that of the waste heat (water) and cooling fluid (water/glycol) circulating pumps and of the air-cooled cooler fans, was taken in consideration. However, on the experimental bench, the total parasitic charges were about 18 kWe (~10 kW for the liquid air-cooled cooler fans, ~3 kW for the hot heat source circulating pump and ~5 kW for the cooling fluid (water/glycol) circulating pump). However, in actual industrial applications, such parasitic power has to be analysed carefully and, if possible, eliminated or substantially reduced. This approach is sometimes possible in practice because many industrial sites are already equipped with waste heat (hot water) and cooling fluids circulating pumps, as well as with cooling towers or other similar cooling devices.

Fig. 7a shows the impact of the waste heat inlet temperature on the net conversion efficiency with cooling fluid inlet temperatures varying from 15 °C to 30 °C. It can be seen that e for example e with the cooling fluid inlet temperature remaining constant at 25 °C, the net conversion efficiency rate increased from 5.1% to 7.5% when the waste heat inlet temperature increased from 85 °C to 115 °C. With waste heat entering the ORC-50 machine at 100 °C, the net conversion efficiency decreased from 7.8% to 4.7% while the cooling fluid temperature increased from 15 °C to 30 °C. Table 3 shows the variation of the energetic net conversion efficiency with the waste heat inlet temperature and cycle temperature increase at a constant cooling fluid inlet temperature (20 °C). It can be seen that the cycle's energetic efficiency increases as the waste heat inlet temperatures and temperature increases move incrementally higher.

On the other hand, the ORC cycle's energetic net conversion efficiency decreased linearly with the environmental weather conditions. Consequently, an ORC machine operating in an area with lower ambient temperature would have better conversion efficiency. The lowest energetic net conversion efficiency (5.5%) was achieved with waste heat inlet temperature of 85 °C and cooling fluid inlet temperature of 30 °C (Fig. 7b). For the same waste heat inlet temperature (85 °C), but with a lower (15 °C) cooling fluid inlet temperature, the net energetic conversion efficiency increased to 6.5%. Thus, with the waste heat inlet temperature remaining constant at 85 °C and 105 °C, the average net conversion efficiency decreased by 15.3% and 14.6%, respectively, when the cooling fluid inlet temperature increased from 15 °C (typical cold climate winter conditions) to 30 °C (summer conditions).

In practice, there are some indirect, but practical, ways to increase the heat-to-power conversion efficiency, even though in practice they will eventually cost more than the value of the additional output. As already shown, one of them consists in increasing the difference between the waste heat water and cooling fluid inlet temperatures, i.e. increasing the cycle temperature lift. Usually, it is difficult to reduce the inlet temperature of the cooling fluid, as this is driven by environmental factors, such as ambient air or water temperatures. On the other hand, there are several techniques to increase the temperature of waste heat coming, for example, from engine exhaust gases by changing the radiator thermostat, or by operating a hot water boiler under pressure with insulated pipes. Also, in the case of ORC machines operating with waste heat at higher temperatures (e.g. >150 °C) by reusing the condensing heat rejected by ORC machines at higher temperatures (up to 49 °C) may provide free waste heat that can generate savings in heating costs and increase overall system efficiency [27].

Table 3
Energetic and exergetic net conversion efficiency as a function of waste heat inlet temperatures and cycle temperature increases.[a]

Test	T^{IN}_{waste} (°C)	$T^{IN}_{waste} - T^{OUT}_{waste}$ (°C)	Net conversion efficiency rate	
			Energetic η_{en} (%)	Exergetic η_{ex} (%)
AD-1	85.8	7.7	6.62	3.95
AD-3	90.8	8.6	6.98	4.11
AD-8	95.6	9.8	7.20	4.29
AD-9	100.3	10.8	7.38	4.38
AD-14	105.5	11.8	7.57	4.43

[a] For variable feed pump speeds at a constant cooling inlet temperature (20 °C).

3.1.3.2. Exergetic conversion efficiency. Irreversibility expresses the net availability (exergy) destruction of the control mass and surroundings, which is proportional to the net entropy increase. The less the irreversibility associated with a given change of state, the greater the amount of work that will be done (or the smaller the amount of work that will be required). The greater the irreversibility we have in all our processes, the greater the decrease will be in our available reserves. It is desirable to accomplish a given objective with the smallest irreversibility. Work costs money, and in many cases a given objective can be accomplished at less cost when irreversibility is lower.

Like the energetic heat-to-electricity net conversion efficiency, the exergetic net conversion efficiency can be defined as

$$\eta_{ex} = \frac{W_{net}}{\dot{E}_{available}} = \frac{W_{net}}{\dot{m}_{waste} e^{IN}_{waste}} = \frac{W_{net}}{Q_{tot-input}\left(1 - \frac{T_a}{T^{IN}_{waste}}\right)} \quad (7)$$

where W_{net} is the net power output (kW), $\dot{E}_{available}$ e the exergy flux available in the waste heat source at the pre-heater/evaporator inlet (kW); $\dot{m}_{waste}$ e the waste heat flow rate (kg/s); e^{IN}_{waste} e the mass exergy of the waste heat carrier fluid entering the cycle (kJ/kg); $(1 - (T_a/T^{IN}_{waste}))$ e the Carnot factor, i.e. the maximum amount of waste heat source which can be transformed into mechanical work; T_a e the ambient absolute temperature (expressed in K) and T^{IN}_{waste} e the waste heat inlet absolute temperature (expressed in K).

By ignoring the potential and kinetic energies, the maximum reversible work per unit mass flow, equal to the decrease in flow availability plus the reversible work that can be extracted from an ORC cycle operating between the waste heat inlet absolute temperature (T^{IN}_{waste}) and the ambient absolute temperature (T_a), is defined as

$$e = (h - h_a) - T_a(s - s_a) \quad (8)$$

The a subscript refers to the dead-state, usually the environment temperature, but here, T_a is the absolute temperature (K) of the cooling fluid entering the condenser of the ORC-50 machine.

Table 3 summarizes both the energetic and exergetic net conversion efficiency rates as a function of the actual waste heat inlet and outlet temperatures (at a constant flow rate of 11.6 kg/s) for a reference ambient temperature of 20 °C equal to the cooling fluid temperature entering the condenser of the ORC-50 machine.

3.2. Impact of superheating

The impact of evaporator superheating on the ORC-50 machine's operating parameters and energy performance was experimentally investigated by setting the feed pump speed to vary between 0 and maximum 37 Hz, while varying the cooling fluid inlet temperatures between 15 °C and 30 °C. By fixing the feed pump speed at maximum 37 Hz, it was found that, with waste heat inlet temperatures higher than 105 °C, this maximum speed became insufficient to keep the evaporator superheating at optimum values (i.e. 4e5 °C). In other words, with waste heat entering the ORC-50 machine at temperatures lower than 105 °C, the speed of the feed pump varied between 0 and 37 Hz and was able to provide optimum superheating amounts for all cooling fluid inlet temperatures provided. However, with waste heat inlet temperatures higher than 105 °C, excessive superheating amounts have been provide because the maximum speed of the feed pump was fixed at 37 Hz. It can be noted that this maximum current frequency wasn't arbitrary chosen, but it was determined after many experimental trials and associated data analysis.

First, it can be seen that with waste heat inlet temperatures above 105 °C and feed pump speed fixed at maximum 37 Hz, the pressure of the superheated vapour at the expander inlet port dropped steeply (Fig. 8a), while the expander inlet temperatures began to increase (Fig. 8b). In order to better illustrate these phenomena, in all the running tests represented in Fig. 8a and b, the cooling fluid inlet temperature was kept constant at 20 °C while the waste heat inlet temperatures varied from 85 °C to 115 °C by 5 °C increments.

Second, by setting the feed pump speed at maximum 37 Hz, the organic fluid flow rate sharply dropped at waste heat inlet temperatures above 105 °C for all cooling fluid inlet temperatures (Fig. 9a). On the other hand, the evaporator superheating reached values as high as 14e19 °C and 23e25 °C with waste heat inlet temperatures of 110 °C and 115 °C, respectively (Fig. 9b). As a direct consequence of reducing the organic fluid flow rate and of excessively increasing the evaporator vapour superheat, the net power output (Fig. 10a) as well as the heat-to-electricity energetic net conversion efficiency rate (Fig. 10b) both stopped increasing at waste heat inlet temperatures above 105 °C, for all cooling fluid inlet temperatures.

4. Cycle improvements

More or less practical and/or theoretical improvements could be made to ORC machines to increase energy performance and reliability. First of all, by appropriately selecting the working (organic) fluids, based on the machine's actual operating conditions, as well as by using an advanced design and selecting the size of the expander, the net conversion efficiency rate may be increased. The working fluids, such as HFC-134a, HFC-245fa, n-pentane and silicon oils, have relatively high critical points and achieve optimal performance in term of cycle efficiency.

Among several alternatives, screw expanders, developed for relatively low-scale ORC machines (<250 kWe), have fixed built-in volume ratios and can use wet fluids with limited superheat at the inlet supply. There are also small screw expanders which can manually or automatically vary the volume ratio within a nearby

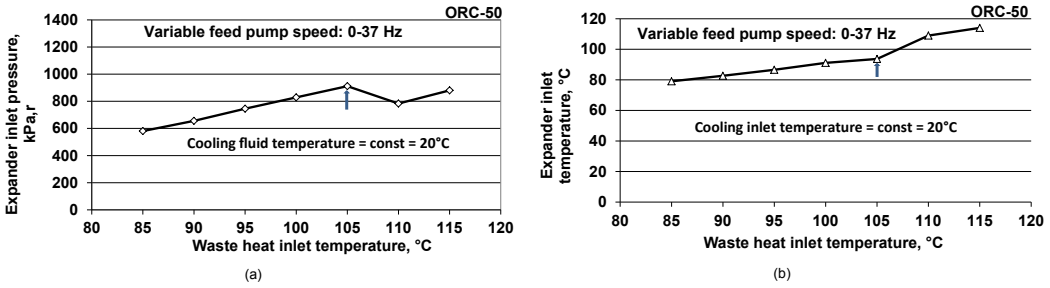

Fig. 8. Expander inlet pressure (a) and temperature (b) as functions of waste heat inlet temperatures, at variable feed pump speed (0e37 Hz) and fixed cooling fluid inlet temperature (20 °C).

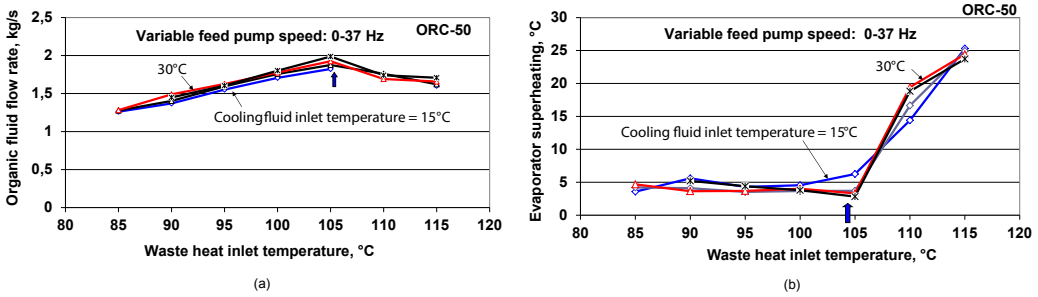

Fig. 9. Organic fluid flow rate (a) and evaporator superheat (b) as a function of waste heat inlet temperatures, at variable feed pump speed (0e37 Hz) and fixed cooling fluid inlet temperature (15 °C).

range to improve efficiency. According to Leibowitz et al. [13], by taking full advantage of the potential of screw expanders, it is possible to produce ORC units for heat recovery from low-temperature heat sources with outputs as low as 50 kW at economically viable costs. However, any risks of oil and/or working fluid leakage through the shaft seal must be limited or avoided.

To improve the net energetic or exergetic conversion efficiency rate of ORC machines, various methods have been proposed, such as using cascade evaporators with high and low-pressure expanders, or two-cycle concepts with fluids having different properties. However, such improvements may significantly increase the initial costs of the systems.

In the case of dry organic fluids entering the expander close to their saturated state (i.e. with small superheat amounts), the cycle can eventually be improved by integrating a regenerator, a counter-current heat exchanger installed between the expander and the condenser. In this cycle, since the fluid does not reach a two-phase state at the end of the expansion process, its temperature is higher than the condensing temperature and it can thus be used to preheat the liquid before it enters the evaporator. Such a process is intended to reduce the thermal power required from the waste heat source to generate the same electrical power, while lowering the overall irreversibility and increasing the conversion efficiency. By using low-temperature heat sources giving at low expander inlet pressures, the amount of waste heat required could be 7.5% lower and the second-law efficiencies of regenerative ORC machines may be approximately 12% higher than those of basic ORC cycles. However, a significant factor in the decision to use or not a regenerator should be the impact of the additional irreversibility in form of pressure drop introduced before the pre-heater and after the expander.

To improve the efficiency and reliability of ORC machines, a number of practical, simple measures have to be carefully applied. First, if high-temperature refrigerants (i.e. refrigerants having relatively high critical temperatures compared to those of conventional ones) are employed as working fluid (e.g. HFC-245fa, of which the critical temperature is 154.05 °C), inlet temperatures of the cooling fluid below certain values (in this example, bellow about 10 °C) must be banned in order to avoid condensing pressures below the atmospheric pressure (vacuum). This situation may eventually allow incondensable gases from the ambient air to enter the system and increase the pressure of the working fluid above its saturation values corresponding to the actual process temperature, whether the machine is running or not. The incondensable gases may also increase the liquid sub-cooling at the condenser outlet as well as the expander outlet pressure and thus reduce the net power output. At lowest waste heat source inlet temperatures (e.g. at 85 °C), the impact may be even higher. By bleeding the liquid receiver prior to each operating period, the overpressures caused by incondensable gases can be drastically reduced and/or eliminated.

Second, before starting the ORC machine, it would be useful to control both the waste (hot) and cooling (cold) fluid flows through the pre-heater/evaporator and condenser, respectively. This precaution may help manage the organic fluid migration within the heat exchangers and other components (expander, liquid receiver, etc.) in order to provide adequate starting sequences.

Third, the feed pump variable speed as well as the expander vapour by-pass and liquid injection have to be carefully controlled during the starting sequences in order to ensure optimum superheating at the evaporator exit and avoid undesirable on/off cycles. For example, during the starting periods it may be helpful to allow the feed pump to run at a given, fixed speed during a certain period of time prior beginning operating at variable speed.

Fourth, in actual industrial applications, the parasitic power consumptions have to be analysed carefully and, if possible, eliminated or substantially reduced. This approach is sometimes possible because many industrial sites are already equipped with waste heat and cooling fluid circulating pumps, as well as with cooling towers or other similar devices.

Finally, for air-cooled ORC systems, the cooling fluid inlet temperature depends on the ambient temperature and cannot be adjusted easily. The challenge consists in finding combined cooling

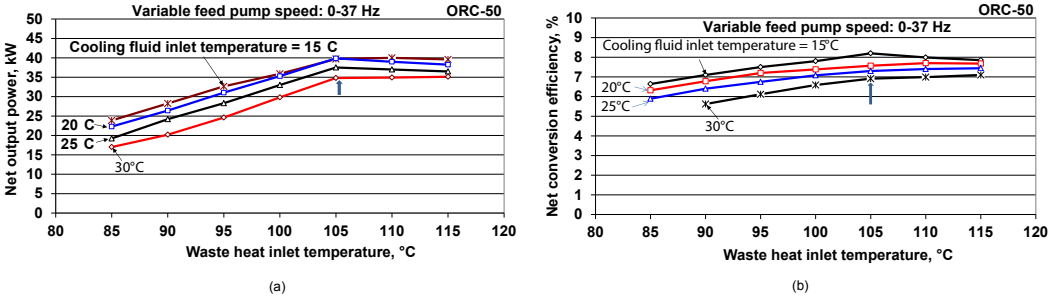

Fig. 10. Net power output (a) and net conversion efficiency rate (b) as a function of waste heat inlet temperatures, at a variable feed pump speed (0e37 Hz) and cooling fluid inlet temperatures at between 15 and 30 °C.

methods for lowering the condensing temperatures during the hottest periods of the year locally.

5. Potential applications

Today, as well as in the future, the challenge is to develop appropriate, performing, and economically feasible industrial applications for ORC machines, especially in countries or markets with high fuel prices and utility capital costs, and/or scarce natural resources.

Leibowitz et al. [13] noted that rising fuel prices, the wide availability of industrial waste heat, and renewable energies (e.g. solar and biomass) open a significant market for ORC machines in small (30e65 electrical kW) and medium (750e1500 kWe) power output ranges, if they could be built and installed at economically competitive prices. Today, the growing need to recover thermal power from industrial low-grade waste heat (or renewable energies) has led to developing systems with initial costs ranging from US$1500 to US$2000 per net electrical kW produced, without any incentives, when parasitic power consumption is ignored [13]. With potential financial incentives and/or for higher output power capacities, the return on the initial investment may accelerate.

The economic competitiveness of ORC machines strongly depends on local energy costs, and therefore their market would be more attractive in those regions of the world with above average electricity prices. Moreover, because turbines may constitute 40e50% of the total cost of conventional steam power plants, inversed compressors and/or expanders have been developed to reduce the cost of this component by up to 90%.

The main applications of ORC machines include heat recovery from high-temperature industrial processes, internal combustion and reciprocating engines (from both jacket cooling water and combustion gas exhaust, up to 1500 kWe/unit), medium size gas turbines, deep geothermal, oil and gas coproduced fluid wells, solar energy sources, biomass boilers (up to 3 MWe/unit), combined heat and power plants, and gas compression stations.

Some high-temperature industrial processes (e.g. aluminium) lose about 50% of the energy used for the electrolytic process, about 2/3 of which is lost through the walls of hundreds of furnaces in each plant and 1/3 from the combustion gases [1]. The energy lost through the walls is difficult to recover, but the heat from electrolysis gases at about 100e130 °C is easier to recover. After filtering and purifying the exhaust gases, the waste heat could be recovered and used for power generation, thus enhancing process efficiency and reducing greenhouse emissions. The power generated may avoid the need to purchase extra electricity to increase aluminium production, and the energy intensity of the process can be reduced and competitiveness improved.

In most of internal combustion engines, only 30e40% of the total fossil thermal heat input is turned into mechanical work, while the remaining 60e70% leaves the engine as waste heat, mainly through the jacket water cooling system and the exhaust pipe. The waste heat from the engine jacket water cooling process (at about 90 °C) is combined with the waste heat from the exhaust gases (at temperatures above 300 °C). Heat is added to the water inside the engine, raising the temperature. The heated water then passes through an exhaust gas heat exchanger, where heat is transferred from the high temperature exhaust into the heated water, increasing the temperature even more. About 10% of these wasted heat sources can be converted into electricity with ORC machines in addition to fulfilling other heating requirements. When fuel costs are high and internal combustion engines are used for electrical production, ORC machines will save fuel costs by allowing the engine to operate at a lower fuel input rate for the same electrical output (Fig. 11a) [9]. Such a heat recovery system, designed and built the exhaust gases of a truck engine, demonstrated its technical feasibility and economical relevance by reducing by 12.5% the fuel consumption [28]. Oomori and Ogino [29] developed an ORC system to recover heat only from the jacket cooling system of an internal combustion engine and Endo et al. [30] proposed a 2.5 kWe ORC machine to recover heat only from the exhaust gases of a 19.2 kWe automotive engine moving at 100 km/h. The heat-to-electricity conversion efficiency was of 13%, while the overall thermal efficiency of the engine increased from 28.9% to 32.7%. These authors suggested that the heat source inlet temperature be controlled by varying the water flow rate through the ORC evaporator with a variable speed pump and that the expander inlet pressure be controlled by varying the rotational speed. Freymann et al. [31] reported on an ORC system recovering heat from both the exhaust gases and jacket cooling fluid.

ORC units can also produce electricity from deep geothermal heat sources at low or medium temperatures ranging between 90 °C and 180 °C. For low-temperature geothermal sources (i.e. below 100 °C) efficiency is relatively low and depends strongly on heat sink temperature that is the ambient air in many applications. Deep geothermal heat sources at temperatures >150 °C enable combined heat and power generation if condensing temperatures are set at higher values (e.g. 60 °C), allowing the cooling water to be used for industrial or space heating. In the case of ORC machines that recover waste heat at temperatures higher than 150 °C, condensing temperatures as high as 60 °C could be achieved. Such temperatures may be efficiently used, for example, for drying biomass and/or preheating the intake air or feed water of biomass boilers, preheating the make-up air of building ventilation systems and/or domestic hot water, and directly using the heat for building radiant floor and swimming pool heating, roadway ice melting and aquaculture of tropical fish species [9]. The heat harnessed by solar collectors can also be converted into electricity through ORC machines. However, solar thermal arrays need thermal storage and have limited periods of operation depending on daylight hours. On the other hand, higher efficiencies can be achieved using parabolic solar collectors combined with Stirling engines. According to Nguyen et al. [32], a solar energy-to-electricity conversion efficiency rate of up to 29.4% has been achieved with a 25 kWe system where the collector temperature reached 750 °C. However, because ORC cycles work at lower temperatures, Fresnel linear concentrators can be used to reduce power plant size and cost. Such an ORC solar plant (1 MWe) installed in Arizona in 2006, using n-pentane as a working fluid, has achieved a 12.1% global solar-to-electricity efficiency rate.

Biomass is another important renewable energy source widely available in a number of industrial processes, such as in the waste and wood industries, that can be used in combined heat and power plants. Biomass is mainly used locally because of its low energy density, which increases transportation costs, and for on-site power demand, which makes biomass suitable for off-grid areas. Biomass boilers are fed with virgin wood chips and thermal oil (mineral or synthetic) at 300 °C within a closed circuit. The single-stage biomass-fired boiler represented in Fig. 11b, the ORC machines can be used because of the lower operating pressure and less stringent legislation compared to steam cycles [27]. The ORC condenser heat can be used as a biomass dryer or for district heating. The boiler cools the thermal oil down to 250 °C, and the turbo-generator produces electrical power with a net efficiency rate of about 18% at full load. At 50% partial load, the net efficiency rate is about 16.5%. Biomass and bio-gases are renewable energy sources for power generation with a net efficiency rate above 16% and high annual operating rates. Biomass is available all over the world and can be used for the production of electricity with small to medium sized scaled power plants. The problem with high specific

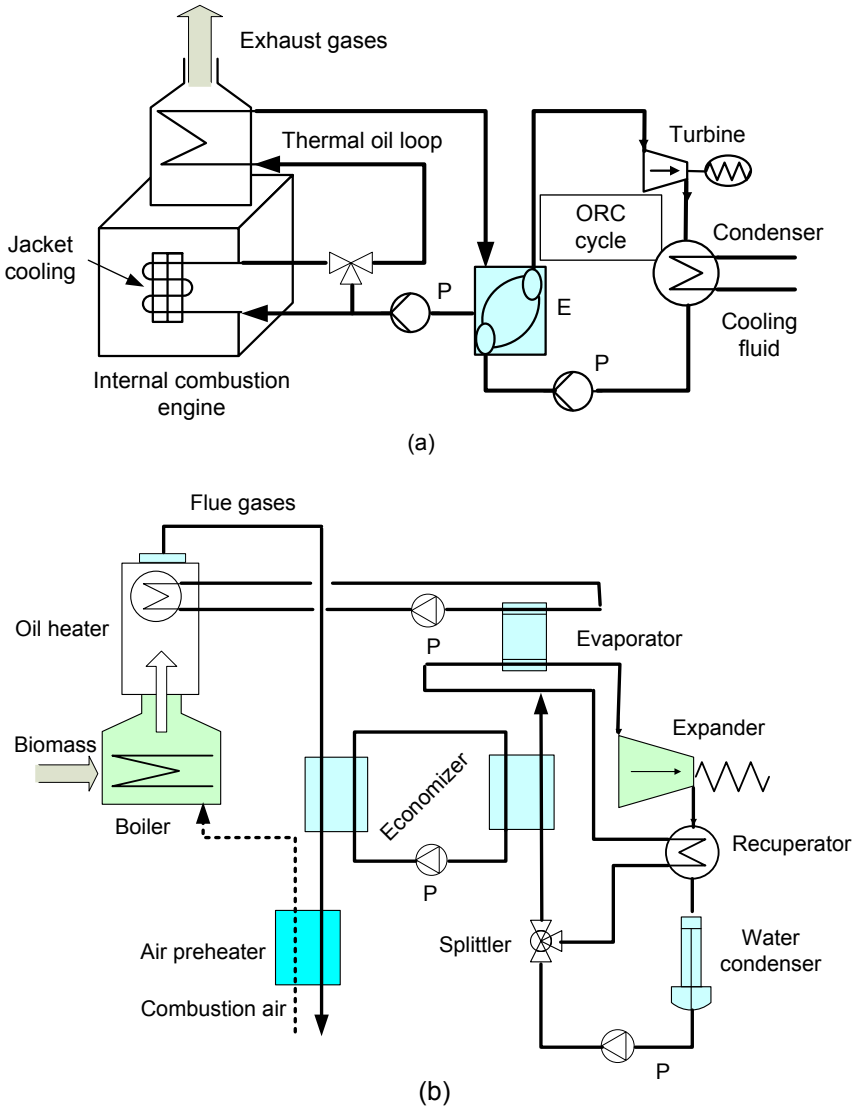

Fig. 11. Schematic representation of heat recovery with ORC machines; (a) from an internal combustion engine [9]; (b) from a biomass boiler with a single-stage ORC combined heating-power system [27].

investment costs for machinery such as steam boilers is overcome thanks to the low working pressures in ORC power plants. The ORC process also helps overcome the relatively small amount of input fuel available in many areas because it is possible to operate a smaller-sized ORC power plant efficiently. ORC units make it possible to generate electric power and heat from the biomass in a simple and efficient manner [9].

In the case of combined heat and power systems, for example, higher flue gas temperature at the outlet of the boiler is required to heat thermal oil to 300 °C. Consequently, to increase the overall energy efficiency of ORC plants, the heat rejected by the condenser must be used for industrial (wood drying, greenhouse and fish farm heating) or district heating, and additional heat exchangers are required to preheat, for example, the ORC working fluid and combustion air. Using waste heat with an ORC system as a bottoming cycle that utilizes the waste heat from the condenser at temperatures above 200 °C may provide a return on investment within two years or even less, which is shorter than with a conventional cycle [27]. Gas compression stations generate a lot of waste heat. A typical gas compression station has many heat sources, some of which need to be cooled (inter-cooling of compressors), so there is a double benefit in both producing electrical power from the heat generated and reducing the cooling power loads on the existing system.

6. Conclusions

This article presents a number of experimental results obtained with a small-scale beta-prototype 50 kWe ORC machine using HFC-245fa as a working fluid. It converts low-grade waste heat or renewable energy at inlet temperatures ranging between 85 °C and 116 °C into electricity, using a cooling fluid at temperatures varying from 15 °C to 30 °C. To achieve superheating amounts lower than 4e5 °C at the evaporator outlet, the speed of the organic fluid feed pump has been set to theoretically vary between 0 and 60 Hz. Under these thermal operating conditions, the net power output and net heat-to-electricity energetic conversion efficiency rate varied between 22.3 kWe and 39.9 kWe, and from 6.62% to 7.57%, respectively. With waste heat inlet temperatures higher than 116 °C, the net conversion factor may reach 10% or more.

This article also confirms that both net power output and energetic conversion efficiency depend on the cooling fluid inlet

temperatures, i.e. on ambient thermal conditions. For example, at the same waste heat source inlet temperature (ex: 90 °C), the expander electrical power output increased by about 28.3% when the cooling fluid inlet temperature dropped from 30 °C to 15 °C. Also, with the waste heat inlet temperature remaining constant at 85 °C and 105 °C, the average net conversion efficiency rate decreased by 15.3% and 14.6%, respectively, when the cooling fluid inlet temperature increased from 15 °C (typical cold climate winter conditions) to 30 °C (maximum summer outdoor temperature). The evaporator superheating impact on the ORC-50 machine's operating parameters and energy performance was experimentally investigated by setting the feed pump speed to vary from minimum 0 and maximum 37 Hz for all waste heat inlet temperatures above 105 °C, while varying the cooling fluid inlet temperatures between 15 °C and 30 °C. By fixing the feed pump speed at maximum 37 Hz, with waste heat inlet temperatures between 105 and 116 °C, excessive superheating amounts (i.e. between 14 and 25 °C) have been recorded. The organic fluid flow rate sharply dropped, as well as the pressure of the superheated vapour at the expander inlet port, while the expander inlet temperatures began to excessively increase. As a consequence of reducing the organic fluid flow rate and of excessively increasing the evaporator vapour superheat, the net power output and the heat-to-electricity energetic net conversion efficiency rate stopped increasing at waste heat inlet temperatures above 105 °C, for all cooling fluid inlet temperatures.

Acknowledgements

The author wishes to acknowledge Hydro-Québec Customer Innovation Department for its support and funding, young scientist researchers Emmanuel Cayer, Marc-André Richard and Éric Le COURTOIS, as well as former Hydro-Québec technician Marcel DÉRY for their outstanding contributions to the project. The author also wishes to acknowledge the North American developer and manufacturer, as well as all local mechanical, electrical and control contractors and engineering firms for their technical support.

Nomenclature

AD	additional
EES	engineering energy solver
GPM	US gallon per minute
HCFC	hydrochlorofluorocarbon
HFC	hydrofluorocarbure
HP	horse-power
kWe	electrical kW
MVA	mega volt Ampere
pre-heat	pre-heater
rpm	rotations per minute
T	temperature (°C or K)

Superscript and subscript

a	ambient
en	energetic
evap	evaporator
ex	exergetic
exp	expander
IN	inlet
OF	organic fluid
OFP	organic fluid feed pump
OUT	outlet
P	pressure
Tot	total

References

[1] Stricker Associates Inc., Market study on waste heat and requirements for cooling and refrigeration in Canadian industry (Main report), 2006.
[2] R.E. Sonntag, C. Borgnakke, G.J. Van Wylen, Fundamentals of Thermodynamics, John Wiley & Sons, 2003.
[3] T. Nugyen, P. Johnson, M. Mochizuki, Design, manufacture and testing of a closed cycle thermosyphon Rankine engine, Heat Recov. Syst. CHP 5 (1995) 333.
[4] F.G. Best, S.B. Riffat, Miniature combined heat and power system, Renew. Energy 6 (1995) 49e51.
[5] J.L. Wolpert, S.B. Riffat, Solar powered Rankine engine for domestic application, Appl. Therm. Eng. 16 (1996) 281e289.
[6] G. Selahattin, Design parameters of a solar-driven heat engine, Energy Sources 18 (1) (1996) 37e42.
[7] T. Yamamoto, T. Furuhata, N. Arai, K. Mori, Design and testing of the organic Rankine cycle, Energy 26 (2001) 239e251.
[8] D.P. DeMarchi, M. Gaia, Performance Analysis of Innovative Collector Fields for Solar-Electric Plants Using Air as Heat Transfer Medium, IEEE, Piscataway, NJ, 1984, pp. 1403e1408, 84CH2101-4.
[9] www.electratherm.com.
[10] V. Minea, Valorisation des rejets thermiques dans les PMI (Rapport synthèse e étape 2, LTE-RS-2011-002.2, avril), 2011.
[11] V. Minea, Production d'énergie électrique avec rejets thermiques industriels, Maîtrise l'énergie 28 (1) (2013) 7e11.
[12] V. Minea, Valorisation des rejets thermiques dans les PMI e étape 3, LTE-RT-2013-0081, Août, 2013.
[13] H. Leibowitz, I.K. Smith, N. Stosic, Cost effective small scale ORC systems for power recovery from low grade heat sources, in: Proceedings of IMECE2006, 2006 ASME International Mechanical Engineering Congress and Exposition, November 5e10, Chicago, Illinois, USA, 2006.
[14] I.K. Smith, N. Stosic, A. Kovacevic, Screw expanders increase output and decrease the cost of geothermal binary power plant systems, GRC Trans. 29 (2005) 787e794.
[15] T.J. Marciniak, J.L. Krazinski, J.C. Bratis, H.M. Bushby, E.H. Buyco, Comparison of Rankine-cycle Power Systems: Effects of Seven Working Fluids (ANL/CNSV-TM-87), Argonne National Laboratory, IL, 1981.
[16] G. Huppmann, Industrial waste heat recovery by use of organic Rankine cycles (ORC), commission of the European communities (Report EUR 9236, 1, Dusseldorf), 1984, p. 409.
[17] S. Manco, N. Nervegna, Working Fluid Selection via Computer assisted Analysis of ORC Waste Heat Recovery Systems, IEEE, Piscataway, NJ, 1985, pp. 71e83.
[18] D.W. Chaudoir, R.E. Niggemann, T.J. Bland, Solar Dynamic ORC Power System for Space Station Application, IEEE, Piscataway, NJ, 1985, pp. 58e65, 85CH2242-6.
[19] ASHRAE Handbook Fundamentals, 2005.
[20] P.H. Snyder, W.C. Moreland, The Selection of Working Fluid Candidates for Use in High Temperature Industrial Heat Pumps (DOE EC-77-C01-5026), Westinghouse Electric Corp., 1978.
[21] R.E. Niggeman, W.J. Greenlee, P.D. Lacey, Fluid Selection and Optimization of an Organic Rankine Cycle Waste Heat Power Conversion System, 1978. ASME 78-WA/Ener-6.
[22] F. Marcuccillli, Electricity Generation from Enhanced Geothermal Systems, September 2006. Workshop 5, Strasbourg, France.
[23] V. Minea, Using geothermal energy and industrial waste heat for power generation, in: IEEE Canada Electrical Power Conference, 2007, pp. 543e549.
[24] N. Stosic, K. Hanjalic, Development and optimization of screw machines with a simulation model, part I: profile generation, ASME Trans. J. Fluids Eng. 119 (September, 1997) 659e663.
[25] K. Hanjalic, N. Stosic, Development and optimisation of screw machines with a simulation model, part II: thermodynamic performance simulation and design, ASME Trans. J. Fluids Eng. 119 (September 1997) 664e670.
[26] N. Stosic, Plural Screw Positive Displacement Machines, 1996. US Patent, 6,296,461.
[27] T.C. Hung, T.Y. Shai, S.K. Wang, A review of organic Rankine cycles for the recovery of low-grade waste heat, Energy 22 (7) (1997) 661e667.
[28] E.F. Doyle, P.S. Patel, Compounding the Truck Diesel Engine with an Organic Rankine Cycle System, Society of Automotive Engineers (SAE), 1976, 760343.
[29] H. Oomori, S. Ogino, Waste Heat Recovery of Passenger Car Using a Combination of Rankine Bottoming Cycle and Evaporative Engine Cooling System, Society of Automotive Engineers (SAE), 1993, pp. 159e164, 930880.
[30] T. Endo, S. Kawajiri, K. Kojima, K. Takahashi, T. Baba, S. Ibaraki, T. Takahashi, M. Shinohara, Study on Maximizing Exergy in Automotive Engines, Society of Automotive Engineers (SAE), 2007, 2007-01-0257.
[31] R. Freymann, W. Strobl, A. Obieglo, The Turbo-steamer: A System Introducing the Principle of Cogeneration in Automotive Applications, vol. 69, 2008, pp. 20e27. MTZ 05/2008.
[32] V.M. Nguyen, P.S. Doherty, S.B. Riffat, Development of a prototype low-temperature Rankine cycle electricity generation system, Appl. Therm. Eng. 21 (2001) 169e181.